

## NOTE

# JBIR-14, a highly oxygenated ergostane, from *Isaria* sp. NBRC 104353

Jun-ya Ueda<sup>1</sup>, Tatsuki Kunoh<sup>2</sup>, Masayuki Sekigawa<sup>2</sup>, Shu-ichi Wada<sup>2</sup>, Yukio Mukai<sup>2</sup>, Shinji Ohta<sup>2</sup>, Ryuzo Sasaki<sup>3</sup>, Tamio Mizukami<sup>2</sup>, Motoki Takagi<sup>1</sup> and Kazuo Shin-ya<sup>4</sup>

*The Journal of Antibiotics* (2010) 63, 139–141; doi:10.1038/ja.2010.3; published online 22 January 2010

**Keywords:** dynAP; ergostane; *Isaria* sp.; Mad2; yeast

Many proteins linked with accelerated proliferation of human cancer cells repress the growth of yeast.<sup>1–3</sup> The inhibitors of these human proteins can restore the inhibition of yeast proliferation with these human proteins, such as Cdk4, PTEN and poly(ADP-ribose) polymerase;<sup>4</sup> therefore, these observations have led to the development of a cell-based high-throughput screening system for anticancer drugs. Our group has revealed that a previously uncharacterized protein, termed dynAP (dynactin-associating protein), inhibits the growth of a mutant budding yeast lacking Mad2, a principal component of mitotic checkpoint, but does not affect the growth of wild-type yeast.<sup>5</sup> DynAP is localized in Golgi and plasma membrane and interacts with dynactin components; it thus forms a complex and acts as a minus end-directed microtubule motor. Furthermore, dynAP expresses in approximately 50% of human cancer cell lines, contrary to its low-level expression in normal cells. Thus, dynAP could be a new target of anticancer drug discovery.

Inhibitors of dynAP could be discovered by monitoring the restoration of dynAP-induced growth inhibition of the mutant yeast lacking Mad2. In the course of our screening program for inhibitors of dynAP, the culture extract of an entomopathogenic fungus, *Isaria* sp. NBRC 104353, exhibited the restoration of dynAP-induced growth inhibition. We isolated a new steroidal compound, named JBIR-14 (**1**), by activity-guided isolation from the culture extract of *Isaria* sp. NBRC 104353 (Figure 1a). We report herein the fermentation, isolation and structure elucidation of **1**.

*Isaria* sp. NBRC 104353, purchased from the National Institute of Technology and Evaluation (Tokyo, Japan), was cultivated in 50 ml test tubes containing 15 ml of potato dextrose broth (24 g l<sup>-1</sup> potato dextrose; BD Biosciences, San Jose, CA, USA). The test tubes were shaken in a reciprocal shaker (355 r.p.m.) at 27 °C for 3 days. Aliquots (1 ml) of the culture were transferred to 100 ml Erlenmeyer flasks

containing a medium consisting of 3 g oatmeal (Quaker, Chicago, IL, USA) and 10 ml V8 Mix Juice (Campbell Soup Company, Camden, NJ, USA) and were incubated in static culture at 27 °C for 14 days.

The culture (20 flasks) was extracted with 80% aq. Me<sub>2</sub>CO. After concentration *in vacuo*, the aqueous concentrate was extracted with EtOAc (100 ml × 3). The organic layer was dried over Na<sub>2</sub>SO<sub>4</sub> and then evaporated to dryness. The dried residue (0.58 g) was subjected to normal-phase medium-pressure liquid chromatography (MPLC; Purif-Pack SI 60 μm, size: 60 (26.5 i.d. × 100 mm), Moritex, Tokyo, Japan) and eluted with a stepwise system of *n*-hexane–EtOAc and CHCl<sub>3</sub>–MeOH, successively, to yield an active fraction (73.0 mg) in CHCl<sub>3</sub>–MeOH (19:1) eluate. The active fraction was rechromatographed on the normal-phase column (Purif-Pack SI 60 μm, size: 20 (20 i.d. × 60 mm) with CHCl<sub>3</sub>–MeOH (99:1, 49:1, successively). Finally, the active fraction (9.5 mg) was purified by preparative reverse-phase HPLC using a Senshu Pak PEGASIL ODS column (20 i.d. × 150 mm; Senshu Scientific, Tokyo, Japan) developed with 80% MeOH–H<sub>2</sub>O including 0.1% formic acid (flow rate: 10 ml min<sup>-1</sup>) to yield **1** (3.4 mg, retention time 19.7 min).

Compound **1** was obtained as a colorless amorphous solid ([α]<sub>D</sub><sup>24</sup> +4.0°, *c* 0.12, in MeOH; UV λ<sub>max</sub> 240 nm, sh, in MeOH) and its molecular formula was determined to be C<sub>28</sub>H<sub>42</sub>O<sub>6</sub> by HR-electrospray ionization-MS (*m/z* 475.3078 [M+H]<sup>+</sup>, calcd for C<sub>28</sub>H<sub>43</sub>O<sub>6</sub>, 475.3060). The IR (ν<sub>max</sub> 1714 cm<sup>-1</sup>) spectra of **1** suggested the presence of a carbonyl group. The direct connectivity between each proton and carbon was established by a heteronuclear single-quantum coherence spectrum. The <sup>13</sup>C and <sup>1</sup>H NMR spectral data for **1** are shown in Table 1. NMR spectra show 28 signals, including six methyl signals (C-18, δ<sub>C</sub> 20.13, δ<sub>H</sub> 1.37; C-19, δ<sub>C</sub> 18.2, δ<sub>H</sub> 0.89; C-21, δ<sub>C</sub> 17.6, δ<sub>H</sub> 1.18; C-26, δ<sub>C</sub> 20.07, δ<sub>H</sub> 0.98; C-27, δ<sub>C</sub> 18.1, δ<sub>H</sub> 0.94; C-28, δ<sub>C</sub> 12.7, δ<sub>H</sub> 0.96). Four partial structures were established by a

<sup>1</sup>Biomedical Information Research Center, Japan Biological Informatics Consortium (JBIC), Aomi, Koto-ku, Tokyo, Japan; <sup>2</sup>Nagahama Institute of Bio-Science and Technology, Tamura-cho, Nagahama-shi, Shiga, Japan; <sup>3</sup>Frontier Pharma, Tamura-cho, Nagahama-shi, Shiga, Japan and <sup>4</sup>Biomedical Information Research Center, National Institute of Advanced Industrial Science and Technology (AIST), 2-4-7 Aomi, Koto-ku, Tokyo 135-0064, Japan. E-mail: k-shinya@aist.go.jp or Dr M Takagi, Biomedical Information Research Center (BIRC), Japan Biological Informatics Consortium (JBIC), 2-4-7 Aomi, Koto-ku, Tokyo 135-0064, Japan.

E-mail: motoki-takagi@aist.go.jp

Received 10 November 2009; revised 4 January 2009; accepted 6 January 2009; published online 22 January 2010

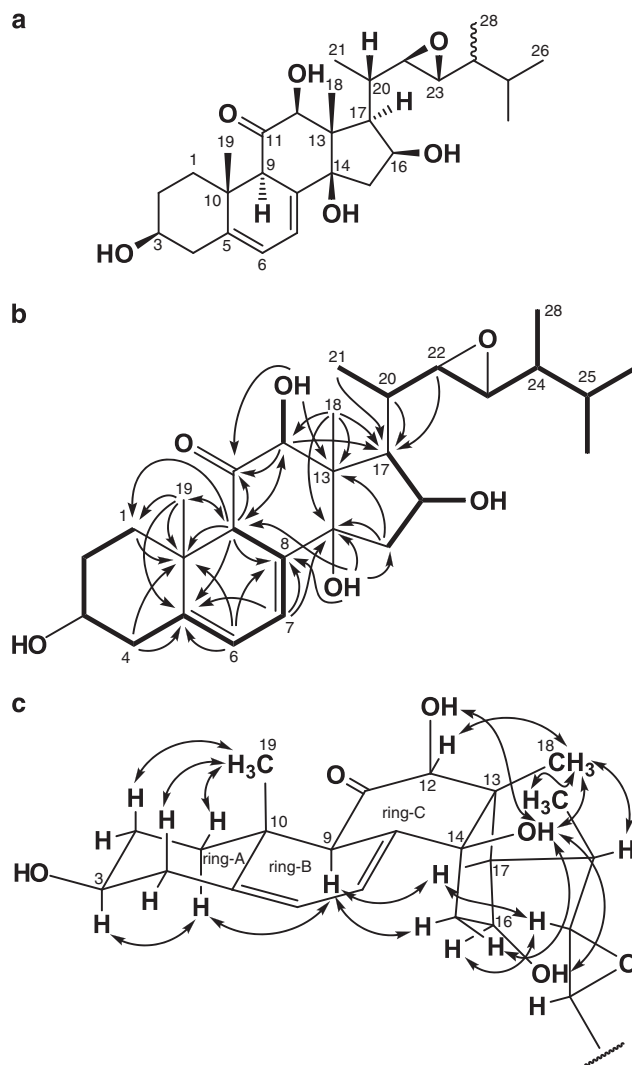


**Figure 1** (a) Structure of **1**. (b) Key correlations of  $^1\text{H}$ - $^1\text{H}$  double-quantum-filtered-COSY (bold line) and heteronuclear multiple bond correlation (arrow, proton to carbon) of **1**. (c) Rotating-frame Overhauser enhancement spectroscopy correlations of **1**.

double-quantum-filtered-COSY spectrum, together with a constant time-heteronuclear multiple bond correlation<sup>6</sup> spectrum as follows:

The sequence from methylene protons 1-H ( $\delta_{\text{H}}$  2.03, 1.55) to a methine proton 9-H ( $\delta_{\text{H}}$  3.06) through methylene protons 2-H ( $\delta_{\text{H}}$  1.93, 1.52), an oxymethine proton 3-H ( $\delta_{\text{H}}$  3.70), methylene protons 4-H ( $\delta_{\text{H}}$  2.52, 2.27), two olefinic protons 6-H ( $\delta_{\text{H}}$  6.33) and 7-H ( $\delta_{\text{H}}$  5.77) including allylic couplings between 4-H and 6-H and between 7-H and 9-H was established as shown in Figure 1b. The  $^1\text{H}$ - $^{13}\text{C}$  correlations from a methyl proton 19-H ( $\delta_{\text{H}}$  0.89) to a methylene carbon C-1 ( $\delta_{\text{C}}$  37.9), an olefinic carbon C-5 ( $\delta_{\text{C}}$  140.1), a methine carbon C-9 ( $\delta_{\text{C}}$  56.8) and a quaternary carbon C-10 ( $\delta_{\text{C}}$  38.4) observed in the heteronuclear multiple bond correlation spectrum of **1** revealed a 9-methyldecalin-2,4(10)-dien-6-ol structure (Figure 1b). The sequence from a methyl proton 21-H ( $\delta_{\text{H}}$  1.18) to a methyl proton 26-H ( $\delta_{\text{H}}$  0.98) through a methine proton 20-H ( $\delta_{\text{H}}$  1.67), two epoxy protons 22-H ( $\delta_{\text{C}}$  62.0,  $\delta_{\text{H}}$  2.80) and 23-H ( $\delta_{\text{C}}$  61.4,  $\delta_{\text{H}}$  2.90), a methine proton 24-H ( $\delta_{\text{H}}$  1.34) and a methine proton 25-H ( $\delta_{\text{H}}$  1.83), together with spin couplings between 24-H and a methyl proton 28-H ( $\delta_{\text{H}}$  0.96) and between 25-H and a methyl proton 27-H ( $\delta_{\text{H}}$  0.94), established a 3,4-epoxy-5,6-dimethylhept-2-yl substructure (Figure 1b). The presence of an oxacyclopropane ring at the positions

of C-22 and C-23 was determined by their characteristic  $^{13}\text{C}$  shifts, and its stereochemistry was determined to be *cis* by their coupling constant ( $J=4.4$  Hz). In a similar manner,  $^1\text{H}$ - $^1\text{H}$  spin couplings for two fragment structures—a hydroxymethine at C-12 ( $\delta_{\text{H}}$  4.10; OH:  $\delta_{\text{H}}$  3.49) and a 2-hydroxypropane composed of 15-H ( $\delta_{\text{H}}$  1.73, 1.62) through 16-H ( $\delta_{\text{H}}$  4.38; OH:  $\delta_{\text{H}}$  4.11) to 17-H ( $\delta_{\text{H}}$  1.53)—were observed as shown in Figure 1b. Long-range couplings from the two methine protons 9-H and 12-H and from the hydroxyl proton 12-OH to a carbonyl carbon C-11 ( $\delta_{\text{C}}$  214.7); from a methyl proton 18-H ( $\delta_{\text{H}}$  1.37) to two methine carbons C-12 ( $\delta_{\text{C}}$  84.3) and C-17 ( $\delta_{\text{C}}$  53.6) and to two quaternary carbons C-13 ( $\delta_{\text{C}}$  58.1) and C-14 ( $\delta_{\text{C}}$  83.7); and from a hydroxyl proton 14-OH ( $\delta_{\text{H}}$  4.48) to C-8 ( $\delta_{\text{C}}$  132.5), C-14 and a methylene carbon C-15 ( $\delta_{\text{C}}$  44.2) elucidated the connectivity among the three substructures, decalin, hydroxymethine and hydroxypropane, in the steroid nucleus. Finally, the remaining 3,4-epoxy-5,6-dimethylhept-2-yl substructure was determined to be attached to C-17 as revealed by  $^1\text{H}$ - $^{13}\text{C}$  long-range couplings from 20-H, 21-H and 22-H to C-17. Thus, the planar structure of **1** was determined as shown in Figure 1a.

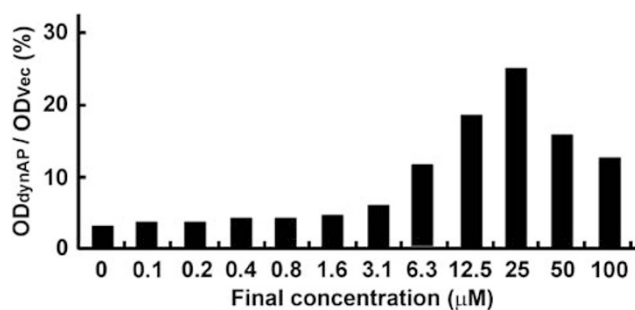
Relative configuration was assigned on the basis of coupling constants and the analysis of a rotating-frame Overhauser enhancement

Table 1  $^{13}\text{C}$  and  $^1\text{H}$  NMR data for **1**

	$\delta_{\text{C}}$	$\delta_{\text{H}}$ (multiplicity, $J$ in Hz)
1	37.9	2.03 (dt, 13.2, 3.1); 1.55 (m)
2	31.3	1.93 (m); 1.52 (m)
3	70.1	3.70 (m)
4	40.2	2.52 (ddd, 14.6, 4.5, 2.3); 2.27 (br d, 13.0)
5	140.1	
6	119.6	6.33 (dd, 5.8, 2.7)
7	119.9	5.77 (dd, 5.8, 2.4)
8	132.5	
9	56.8	3.06 (br s)
10	38.4	
11	214.7	
12	84.3	4.10 (d, 4.7)
13	58.1	
14	83.7	
15	44.2	1.73 (br d, 14.2); 1.62 (m)
16	75.8	4.38 (dt, 3.4, 2.9)
17	53.6	1.53 (m)
18	20.13	1.37 (s)
19	18.2	0.89 (s)
20	30.4	1.67 (m)
21	17.6	1.18 (d-like, 6.6)
22	62.0	2.80 (dd, 9.6, 4.4)
23	61.4	2.90 (dd, 9.8, 4.4)
24	36.4	1.34 (m)
25	31.1	1.83 (septet of doublet, 6.9, 4.4)
26	20.07	0.98 (d, 7.1)
27	18.1	0.94 (d, 6.8)
28	12.7	0.96 (d, 6.8)
12-OH		3.49 (d, 4.9)
14-OH		4.48 (s)
16-OH		4.11 (br s)

NMR spectra were measured on a Varian NMR system 500 NB CL (Varian, Palo Alto, CA, USA) in chloroform-*d* with the residual solvent peak as an internal standard ( $\delta_{\text{C}}$  77.0,  $\delta_{\text{H}}$  7.26 p.p.m.).

spectroscopy experiment. The large coupling constants for  $J_{2\beta\text{H},3\text{H}}$  (11.0 Hz) and  $J_{3\text{H},4\beta\text{H}}$  (11.0 Hz) and for the rotating-frame Overhauser enhancement spectroscopy correlations (Figure 1c) between 1- $\alpha\text{H}$  and 3-H; between 2- $\beta\text{H}$  and 19-H; and between 4- $\beta\text{H}$  and 19-H indicated that ring-A should be in a chair conformation with the hydroxyl groups at C-3 in  $\beta$ -equatorial orientation and with the methyl group (C-19) at C-10 in  $\beta$ -axial orientation. On the other hand, the rotating-frame Overhauser enhancement spectroscopy correlations between 1- $\alpha\text{H}$  and 9-H; between 9-H and 15- $\alpha\text{H}$ ; and between 9-H and 17- $\alpha\text{H}$  revealed that the ring junction proton 9-H is located in  $\alpha$ -axial orientation. Further, the rotating-frame Overhauser enhancement spectroscopy correlations between 12-H and 18-H; between 12-OH and 14-OH; between 14-OH and 18-H; between 14-OH



**Figure 2** Recovery of the dynAP-induced growth inhibition of Mad2-lacking mutant yeast by **1**. Exponentially growing Mad2-lacking mutant cells harboring the empty vector or dynAP expression vector were washed and adjusted for their cell density, followed by incubation in galactose medium containing **1** in DMSO or DMSO alone. After 48 h, growth recoveries were calculated by measuring the OD of cell cultures.  $\text{OD}_{\text{vec}}$  is OD of mutant cells harboring the empty vector treated with DMSO.  $\text{OD}_{\text{dynAP}}$  is OD of dynAP-expressed mutant treated with **1**.

and 15- $\beta\text{H}$ ; between 14-OH and 16-OH; between 18-H and 20-H; and between 18-H and 21-H revealed that the three hydroxyl groups at C-12, C-14 and C-16, the methyl group (C-18) at C-13 and the side chain at C-17 are in  $\beta$ -orientation, but that of C-28 was not determined. Thus, the structure of **1** was established as (3 $\beta$ ,12 $\beta$ ,14 $\beta$ ,16 $\beta$ )-22,23-epoxy-3,12,14,16-tetrahydroxyergosta-5,7-dien-11-one (Figure 1).

Compound **1** restored the dynAP-induced growth inhibition of Mad2-lacking mutant yeast at a concentration of 25  $\mu\text{M}$  (Figure 2). Furthermore, compounds related to **1** induced dynAP-mediated Golgi fragmentation and apoptosis in human cancer cells.<sup>5</sup> Thus, **1** may serve as an important compound for developing anticancer drugs and also as a valuable tool for conducting studies on the action mechanism of dynAP. The detailed biological activity and the structure–activity relationship of **1** will be reported elsewhere.<sup>5</sup>

## ACKNOWLEDGEMENTS

This study was supported by a grant from the New Energy and Industrial Technology Department Organization (NEDO) of Japan.

- 1 Moorthamer, M., Panchal, M., Greenhalf, W. & Chaudhuri, B. The p16(INK4A) protein and flavopiridol restore yeast cell growth inhibited by Cdk4. *Biochem. Biophys. Res. Commun.* **250**, 791–799 (1998).
- 2 Cid, V. J. *et al.* Assessment of PTEN tumor suppressor activity in nonmammalian models: the year of the yeast. *Oncogene* **27**, 5431–5442 (2008).
- 3 Perkins, E. *et al.* Novel inhibitors of poly(ADP-ribose) polymerase/PARP1 and PARP2 identified using a cell-based screen in yeast. *Cancer Res.* **61**, 4175–4183 (2001).
- 4 Simon, J. A. & Bedalov, A. Yeast as a model system for anticancer drug discovery. *Nature Rev. Cancer* **4**, 481–492 (2004).
- 5 Kunoh, T. *et al.* Identification of a novel human dynactin-associated protein, dynAP, and chemicals that induce dynAP-mediated apoptotic cell death (In submission).
- 6 Furihata, K. & Seto, H. Constant time HMBC (CT-HMBC), a new HMBC technique useful for improving separation of cross peaks. *Tetrahedron Lett.* **39**, 7337–7340 (1998).